# 6q- is an early and persistent chromosomal aberration in CD3⁻CD4⁺ T-cell clones associated with the lymphocytic variant of hypereosinophilic syndrome

Marie Ravoet
Catherine Sibille
Florence Roufosse
Hugues Duvillier
Christos Sotiriou
Liliane Schandené
Philippe Martiat
Michel Goldman
Karen E. Willard-Gallo

Background and Objectives. The lymphocytic variant of hypereosinophilic syndrome (LV-HES) is an underrated disease defined by the monoclonal proliferation of interleukin-5 secreting T-cells. This disease is distinguished by a period of chronic lymphoproliferation without clinical transformation, which is frequently a precursor to T-cell lymphoma. In this study, LV-HES was used as a model of pre-malignancy to identify specific marker(s) predictive of the potential for malignant transformation.

Design and Methods. The karyotypic abnormalities detected in the abnormal CD3⁻CD4⁺ T cells were further characterized by fluorescent *in situ* hybridization. A multi-step retrospective analysis was performed on successive blood samples during a six-year follow up to correlate the evolution of cytogenetic changes with clinical progression. Expression array analysis was used to investigate the effect of these chromosomal aberrations on gene expression.

Results. A 6q deletion was detected in the two LV-HES patients during their chronic disease phase. An additional 10p deletion was found alone or in association with the 6q defect in one patient prior to the development of a CD3⁻CD4⁺ T-cell lymphoma six years after diagnosis. We show that the 6q but not the 10p deletion is both stable and persistent throughout the chronic disease, finally emerging as the predominant aberration in the lymphoma cells. Six genes mapped to the 6q-deleted region displayed altered gene expression profiles both in the chronic and malignant disease phases.

Interpretations and Conclusions. Our data suggest that the 6q deletion represents an early cytogenetic marker for T-cell transformation.

Key words: hypereosinophilic syndrome, 6q, pre-malignancy, CD3⁻CD4⁺ T-cell lymphoma, expression profile.

Haematologica 2005; 90:753-765



*From the Center for Human Genetics UCL, Cliniques Universitaires St Luc UCL, Brussels, Belgium (MR, CS); Departments of Immunology and Internal Medicine, Hôpital Erasme, Université Libre de Bruxelles, Brussels Belgium (FR, LS, MG); Laboratory of Experimental Hematology, Institut Jules Bordet, Université Libre de Bruxelles, Brussels, Belgium (MR, HD, CS, PM, KEW-G).*

*Correspondence:*
*Dr. Catherine Sibille, Center for Human Genetics UCL, GMED, Cliniques Universitaires St. Luc, Avenue E. Mounier 10-F 1200 Brussels, Belgium*
*E-mail: catherine.sibille@gmed.ucl.ac.be*

Cytogenetic analysis recurrently detects a 6q deletion in lymphoid malignancies, including both T- and B-cell acute lymphoblastic leukemia (ALL)[1-3] and non-Hodgkin's lymphoma (NHL).[3-5] Interestingly, this abnormality has rarely been reported in myeloid leukemia.[6] A variety of solid tumors such as melanoma,[7] breast carcinoma[8] and prostate cancer[9] have also been shown to exhibit the same defect. The recurrence of a 6q deletion in cancer strongly suggests that this region contains an unidentified tumor-suppressor gene(s) and therefore merits further investigation for its role in the malignant process. This hypothesis is supported by studies showing that tumorigenicity can be suppressed by introducing all or part of a normal chromosome 6 into immortalized fibroblasts, ovarian or breast cancer cell lines.[10,11]

The idiopathic hypereosinophilic syndrome (HES) is a heterogeneous group of diseases defined by a persistent blood hypereosinophilia of unknown etiology leading to tissue damage.[12] Two distinct types of HES have emerged from this pathologic group: the myeloid variant related to chronic eosinophilic leukemia[13] and the lymphocytic variant of hypereosinophilic syndrome (LV-HES). The latter is characterized by a monoclonal expansion of peripheral helper T cells overexpressing Th2-type cytokines, including interleukin (IL)-4 and IL-5, the likely cause of the hypereosinophilia *in vivo*.[14-24] The monoclonal T cells are often distinguished by an aberrant surface immunophenotype, which is most frequently either CD3⁻CD4⁺CD8⁻[14,15,19,21] or CD3⁺CD4⁻CD8⁻.[16,17] Disease progression is usually characterized by a long chronic phase associated with cutaneous manifestations and a favorable prognosis. However, some LV-HES patients subsequently develop a T-cell lymphoma originating from the same abnormal T-cell clone. This suggests that these cells possess a potent pre-malig-

nant nature early in the disease process.[18,20,23] A prognostic marker for the malignant potential of these abnormal T cells has not yet been identified, but cytogenetic analysis is a powerful tool routinely used for the diagnosis and prediction of prognosis in malignant hematologic disorders. We therefore initiated a retrospective analysis of the progressive chromosomal aberrations present in the $CD3^-CD4^+$ T-cell clones from two LV-HES patients (initial case reports previously described).[21] A 6q deletion was detected early and persisted throughout the chronic disease phase in both individuals, emerging as the predominant genetic anomaly in one patient in concert with progression of her disease to T-cell lymphoma. Gene expression array analysis was employed to investigate the impact of this deletion on the expression of 6q located genes, and six of the 88 genes examined were found to be consistently downmodulated in the $CD3^-CD4^+$ T cells from both patients.

## Design and Methods

### Patients

The initial clinical presentation of patients 1 and 2 has been previously described[21] where they are also indicated as P1 and P2, respectively. Briefly, at initial diagnosis patient #1 (a 20-year old female) exhibited severe cutaneous manifestations (eczema, pruritis, tenosynovitis of the right ankle). The circulating leukocyte count was $16.9\times10^9$/L with $8.92\times10^9$/L eosinophils and $4.63\times10^9$/L lymphocytes, including $3.45\times10^9$/L $CD3^-CD4^+$ T cells. A four-year follow-up was marked by episodes of severe eczema treated with corticosteroids and/or interferon (IFN)-α. Four years after diagnosis, her circulating leukocyte count had reached $26.2\times10^9$/L, with $17.08\times10^9$/L eosinophils and $6.32\times10^9$/L lymphocytes, including $4.80\times10^9$/L $CD3^-CD4^+$ T cells, and the clinical manifestations had worsened. Six cycles of fludarabine were administered, after which she achieved clinical remission for a few months characterized by a steadily declining number of aberrant T cells in the peripheral blood. The circulating leukocyte count was $1.2\times10^9$/L, including $0.2\times10^9$/L eosinophils and $0.38\times10^9$/L lymphocytes ($0.1\times10^9$/L $CD3^-CD4^+$ T-cells). However, six years after the initial diagnosis, the patient relapsed. Enlarged lymph nodes were detected in the pre-auricular, cervical, and inguinal regions, and a histological diagnosis of peripheral diffuse T lymphoma of small to medium lymphocytes, type 4 (Class II, REAL/peripheral T lymphoma, WHO) was established. The leukocyte count was $15.1\times10^9$/L, with $8.61\times10^9$/L eosinophils and $4.0\times10^9$/L lymphocytes, including $2.93\times10^9$/L $CD3^-CD4^+$ T cells. After a six-month course of CHOP-like chemotherapy, and, although lymph node size decreased, $CD3^-CD4^+$ T cells remained detectable and hypereosinophilia persisted. Three months later the patient was successfully treated by allogeneic stem cell transplantation from a family donor and is currently in complete remission.

At initial diagnosis patient 2 (a 21-year old female) exhibited cutaneous symptoms. The total leukocyte count was $14.8\times10^9$/L, including $9.1\times10^9$/L eosinophils and $3.42\times10^9$/L lymphocytes ($2.47\times10^9$/L $CD3^-CD4^+$T cells). A four-year follow-up on continuous low-dose corticosteroid therapy has been characterized by remission of symptoms, decreased eosinophilia ($0.6\times10^9$/L) and a significant decrease in the $CD3^-CD4^+$ T cell population to $0.09\times10^9$/L (leukocyte count was $7.2\times10^9$/L, including $0.66\times10^9$/L eosinophils and $1.42\times10^9$/L lymphocytes).

### Cell purification

Circulating leukocytes were obtained from patients and from healthy female donors (25-30 years old) either by venipuncture in 60-mL heparinized syringes or by cytapheresis. Peripheral blood mononuclear cells (PBMC) were isolated and either used for immediate processing or frozen as described.[21] If necessary, PBMC were thawed and cultured overnight in supplemented RPMI 1640 without stimulation. The next morning, the $CD2^+CD3^-CD4^+$ and $CD2^+CD3^+CD4^+$ T-cell populations were purified by flow cytometry on a Beckman-Coulter Elite. PBMC were resuspended in RPMI 1640 without phenol red supplemented with 5% decomplemented fetal bovine serum and labeled with fluorescein-isothiocyanate (FITC)-coupled anti-CD2 monoclonal antibody (Moab) (Clone Leu-5b, BD Biosciences), phycoerythrin (PE)-coupled anti-CD4 Moab (Clone 13B8.2, Beckman Coulter) and phycoerythrin-cyanin5 (PC5)-coupled anti-CD3 Moab (Clone UCHT1, Beckman Coulter). The purity of sorted T-cell populations was analyzed on a FACS Calibur (BD). Moreover, the abnormal $CD3^-CD4^+$ and normal $CD3^+CD4^+$ T-cells were also purified by magnetic beads. The $CD4^+$ T cells were first isolated from PBMC by column depletion using the MACS $CD4^+$ T-cell isolation kit according to manufacturer's instructions (Miltenyi Biotech, Bergisch Gladbach, Germany). The isolated $CD4^+$ T cells were then labeled with anti-CD3 Moab coupled magnetic microbeads (Miltenyi Biotec) and the $CD3^-CD4^+$ and $CD3^+CD4^+$ T-cell populations were differentially separated on a magnetic column (Miltenyi Biotec). The purity of these T-cell populations was checked, as described above.

### Metaphase cells, preparation of nuclei and karyotyping

Metaphase cells were prepared from fresh peripheral blood samples or T-cell cultures for standard karyotyping[25] by stimulating them for 72 hours with 20

μg/mL phytohemagglutinin (PHA; Life Technologies, Merelbeke, Belgium) and/or 100U/mL recombinant human IL-2 (Cetus Corp., Emeryville, CA, USA). The metaphase cells used in the FISH experiments were obtained from thawed PBMC that were subsequently stimulated for 5 days with a combination of recombinant human IL-2 (100U/mL), anti-CD28 antibody (1 μg/mL; Clone 28.2, Immunotech) and phorbol-12-myristate-13-acetate (PMA; 1ng/mL; Calbiochem, Leuven, Belgium) and were stopped in metaphase by adding colcemid (25 ng/mL; Life Technologies). The nuclei for interphase FISH were obtained either from unstimulated thawed PBMC or from sorted T-cell populations, as described above.

### PAC (P1 derived artificial chromosome) and BAC (bacterial artificial chromosome)

All PAC and BAC clones were selected in the Sequence Maps from the National Center for Biotechnology Information (NCBI) and purchased from the Children's Hospital Oakland (available at URL *http://www.chori.org/bacpac*). The chromosome 6-located PAC clones included: RP1-22I17 (at 6q12), RP1-91B17 (at 6q12), RP1-104A17 (at 6q13), RP3-424L16 (at 6q13), RP1-234P15 (at 6q14.1), RP3-429G5 (at 6q21), RP1-238J17 (at 6q22.1), RP1-136O14 (at 6q22.1), RP3-412I7 (at 6q22.1), RP1-193N13 (at 6q22.31) and RP1-293L8 (at 6q22.32). An additional RP3-324N14 PAC clone (at 6q23.1) was kindly provided by Frédéric Chibon (Institut Curie, Paris, France). The chromosome 10-located BAC clones included: RP11-462L8 (at 10p11.22), RP11-271M1 (at 10p13), RP11-2K17 (at 10p13), RP11-398C13 (at 10p13) and RP11-20J15 (at 10q11.21). The clones were grown and the DNA isolated using standard molecular biology techniques. The identities of PAC and BAC clones were verified using FISH to examine the correct chromosomal location or by DNA sequencing and matching to the sequences in the NCBI database.

### Fluorescence in situ hybridization

FISH experiments were performed using previously described protocols.[26] Briefly, PAC/BAC and α-satellite centromeric plasmid D6Z1 and D10Z1, specific for centromeres of chromosomes 6 and 10 (kindly provided by Pr A. Hagemeijer, KUL) were labeled with either tetramethylrhodamine-5-dUTP or fluorescein-12-dUTP (Roche Applied Science, Mannheim, Germany) by nick-translation. The labeled probes were denatured in hybridization buffer containing ultrapure formamide (Life Technologies) and PAC/BAC probes were pre-hybridized for 30 minutes. Hybridization was carried out on RNase-treated nuclei or mitotic slides using 50 ng/μL of PAC/BAC and, if necessary, 4 ng/μL of centromeric probes and hybridization was processed in a moist chamber overnight at 37°C. After a post-hybridization wash carried out at 30°C for 2 minutes in a 0.4× SSC bath, the slides were counterstained with 4,6-diamidino-2-phenylindole dihydrochloride (DAPI) in an anti-fade solution (Vectashield, Vector Laboratories, Burlingame, CA, USA). Hybridized slides were examined using either a DMRB microscope (Leica) or an axioplan 2 microscope (Zeiss) and images were captured using a Photometrics camera and processed by SmartCapture software (Digital Scientific, UK).

In addition, successive dual color FISH hybridization/slide washing cycles of mitotic slides were carried out as described in[26] with an additional wash in Carnoy's solution for 2 minutes before the hybridization.

In interphase FISH experiments, only dual-color FISH was performed using a FITC-labeled specific PAC/BAC probe with a rhodamine-labeled centromeric probe (either D6Z1 or D10Z1, according to the 6q- or 10p-specific probe, respectively) as an internal control for disomy. The interphase FISH results were obtained by counting >500 intact nuclei per patient slide. The cut-off level for each probe was determined by scoring 200 intact nuclei prepared from PBMC and $CD3^+CD4^+$ T cells purified from five healthy donors used to set the baseline based on the mean plus three standard deviations. The thresholds of detection on unsorted nuclei were 4% for RP1-234P15, RP1-238J17 and RP3-424L16, 5% for RP1-91B17, RP1-136O14, RP3-412I7, RP3-429G5 and RP11-462L8 and 7% for RP1-193N13. The thresholds of detection on sorted cells were 6% for RP11-462L8, 7% for RP1-193N13, 8% for RP1-91B17 and 9% for RP3-429G5.

### RNA purification

Total RNA was isolated from sorted T cells using TriPure Isolation Reagent (Roche Applied Science) in a single-step extraction method.[27] The quality of the RNA was assessed using the Agilent Capiler system. If required, samples of equal amounts of total RNA were pooled.

### Oligonucleotide microarray

Total RNA (2-3 μg) was labeled using the BioArray High Yield RNA Transcript Labeling Kit (Enzo Biochem, New York, NY, USA) following the manufacturer's standard procedures (Affymetrix, Santa Clara, CA, USA). The labeled cRNA were hybridized on test3arrays (Affymetrix) to ensure the quality of the probes. The probes were recovered and hybridized on U133A Genechips, containing 22,263 probe sets. The hybridization, washing, staining and scanning of the array slides were performed according to standard protocols (Affymetrix). Gene expres-

sion values from the CEL files were normalized using RMA.[28] Biological replicate experiments were performed for each purified T-cell population. The data were interpreted by sorting for robust changes in pair-wise comparisons as described in the GeneChip expression analysis manuals (Affymetrix).

### Reverse transcription and quantitative real-time PCR (RQ-PCR)

Standard reverse transcription was performed using 200 ng-1 μg of total RNA, random hexanucleotides (50 μM final concentration, Amersham Pharmacia, Freiburg, Germany), MMLV reverse transcriptase (100 U, Promega, Leiden, The Netherlands) and RNase inhibitor (20 U, Promega). After denaturing the RNA, the RT-PCR reaction was performed for 45 minutes at 42°C followed by an enzyme-inactivation step. Next, 25 ng of cDNA were subjected to a real-time PCR reaction using 2× SYBR Green PCR Master Mix (Applied Biosystems, Lennik, Belgium) and 0.32 μM each of the gene-specific forward and reverse primers (Life Technologies). The following primers were designed using the Primer Expression 1.0 program (Applied Biosystems):

FOXO3A/ex3-F: 5'-CATGGGCCATGAGAAGTTCC-3'
FOXO3A/ex3-R: 5'-CATGTCACATTCCAAGCTCCC-3'
FOXO3A/ex4-F: 5'-TGCATAGGCAAAAGGAGTGGA-3'
FOXO3A/ex4-R: 5'-GATCACCCTGACTCAGAACCG-3'
C6ORF37-F: 5'-ACTGCAATGTGCTGAACTGGG-3'
C6ORF37-R: 5'-TGAATCGGAATGGTCTCGCT-3'
PA26-F: 5'-CCTCGACCACTAGGACAGGG-3'
PA26-R: 5'-GTGCGTCTTCACTCCCCACT-3'
MARCKS-F: 5'-CCACAGATCCCATCTCAAATCAT-3'
MARCKS-R: 5'-AGAGAAACAAGGCAGAGGAAGAAG-3'
CD164-F: 5'-TTGACTGAGCGTTGCGAGC-3'
CD164-R: 5'-AGAGCCGCGACATCGTGT-3'
HMGN3-F: 5'-CCAAAGTAACTAAACAGGAGCCCA-3'
HMGN3-R: 5'-GTTCAGGTTTTGGTGGAGCAG-3'
ORC3L-F: 5'-TCAGTGCTGCCCATGCC-3' x
ORC3L-R: 5'-AAGGATTGTTGAGTGCAGTATGGA-3'
SUSP1-F: 5'-TTTCTTCAAGCAATTCCAGCAGT-3'
SUSP1-R: 5'-CCTTTACAATCATTCCAAACTTTATCC-3'
PROL2-F: 5'-GCCTGAGAAGTGGAGATTGCA-3'
PROL2-R: 5'-TGAGACAGCGTCTGTTACCCAG-3'
BACH2-F: 5'-CAGCAATACTGTTCCGAAGTATCCT-3'
BACH2-R: 5'-GTGTCATCACTGCTGTCTTTCCTT-3'
C6ORF162-F: 5'-AAACAAAGCCTAGCCCTACGGT-3'
C6ORF162-R: 5'-CGGGCCAGGTGCCAG-3'

The *ABL* gene was used as an endogenous control.[29] Standard real-time PCR was performed on an ABI Prism 7900 HT (Applied Biosystems). Dissociation curves were verified and the PCR products were visualized on 1.5% agarose gel to ensure the specificity of the PCR reaction. The amplified fragments were then isolated using the QIAquick Gel Extraction kit (Qiagen) and a series of dilutions were prepared to generate the standard curves for reproducibility and efficiency of the reactions. All real-time PCR reactions were processed in duplicate and differences of more than 1 Ct were rejected. The comparative Ct method was applied for data analysis. For all tested genes, biological duplicates were performed, with a third biological replicate analyzed for the *C6ORF37*, *HMGN3*, *MARCKS*, *PA26*, *RAGD* and *SUSP1* genes.

## Results

### T-cell receptor rearrangements

Samples from both patients were examined annually for rearrangement of their T-cell receptor (TCR) γ chain gene (*TCRG*) by PCR. A clonal *TCRG* rearrangement was routinely detected in both whole blood and isolated $CD3^-CD4^+$ T cells from patients 1 and 2 (P1 and P2). The aberrant mature T-cell phenotype and cytokine profile associated with the $CD3^-CD4^+$ T-cell clone in both patients[21] (*Willard-Gallo et al., submitted to Exp Hematol*) led us to analyze the *TCRB* locus. Using IL-2-dependent $CD3^-CD4^+$ T-cell lines derived from P1 at diagnosis (*Willard-Gallo et al., submitted to Exp Hematol*), we established that these cells had a clonally rearranged *TCRB* gene using Southern blotting (Figure 1). On the basis of our results with the cell lines, we examined sequential whole blood samples from both patients and found that *TCRB* gene rearrangements became detectable three years after diagnosis for P1 (Figure 1) and two years after diagnosis for P2 (data not shown). The clonal *TCRB* rearrangement detected in the blood of P1 was identical to that found in the P1-derived $CD3^-CD4^+$ T-cell lines, indicating that the cells grown *in vitro* accurately reflected the abnormal $CD3^-CD4^+$ T cells present *in vivo*. The presence of a completely rearranged *TCRB* gene in conjunction with the phenotype and cytokine profile of the $CD3^-CD4^+$ T cells indicates the abnormal clone was derived from a mature T cell.

### Karyotype of the $CD3^-CD4^+$ T--cells from patient #1

The abnormal surface phenotype and cytokine profiles characteristic of the $CD3^-CD4^+$ T cells were not reflected by an aberrant cellular morphology in either P1 or P2. We therefore examined these cells for potential cytogenetic abnormalities. At initial diagnosis, fresh blood cells from patient #1 appeared to be normal by conventional karyotyping (G-banding, 72-hour PHA stimulation). Once again we stimulated the cell line from patient #1 using IL-2, and although these cultured lines (100% $CD3^-CD4^+$) contained some cells with a normal karyotype, the large majority had abnormalities easily detected by conventional karyotyping. The most frequent aberration identified was a 6q deletion, present either as a unique abnormality (the $6q^-$ subclone) or in association with a 10p deletion (the $6q^-10p^-$ subclone), with an addi-

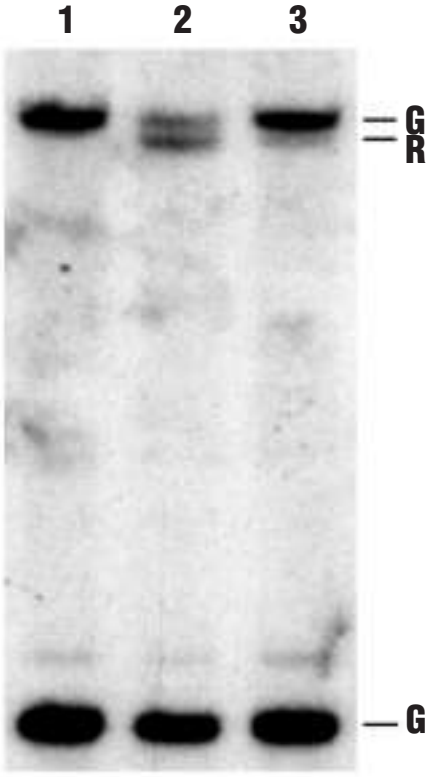


Figure 1. *TCRB* gene clonality. Southern blot analysis of the *TCRB* gene: *lane 1*, a peripheral blood sample from a healthy control; *lane 2*, long-term cultures of CD3$^-$CD4$^+$ T cells from P1 and *lane 3*, a peripheral blood sample from P1. The germline (G) configuration only is detected in the control, whereas in P1's samples an additional rearranged (R) band is present. DNA was digested with *EcoR*I and hybridized with a Jβ2 specific probe as described.[22]

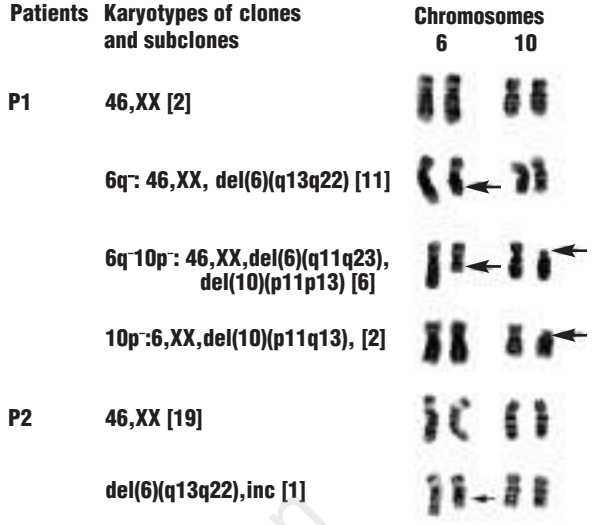


Figure 2. The G-banded karyotypes from P1 and P2 in long-term cultures. The karyotypes obtained from long-term cultures (100% pure CD3$^-$CD4$^+$ T cells) of blood samples drawn at initial diagnosis from P1 and P2. Chromosomes 6 and 10, representative of each clone and subclone, are also shown.

tional subclone possessing the 10p abnormality alone (the 10p$^-$ subclone) (Figure 2). The same cytogenetically abnormal subclones were eventually found to be present in fresh blood from patient #1, but again not until three years after initial diagnosis despite routine annual karyotyping. This suggests that the 6q and 10p abnormalities were not an artifact of *in vitro* cell culture, but instead were undetectable by the standard assays used in routine clinical analysis. Using PHA and IL-2 to stimulate these cells enabled us to consistently detect the presence of the abnormalities in the patient's blood except on a single occasion that was concurrent with fludarabine-induced remission. The *TCRB* and karyotypic analyses demonstrate the usefulness of *in vitro* cell culture as a means of expanding and examining abnormal cell clones that either have a low proliferative capacity or are present at low frequency in the early stages of a given disease.

### *Karyotype of the CD3$^-$CD4$^+$ T cells from patient 2*

The analysis of fresh blood cells from P2 at initial diagnosis once again revealed only a normal karyotype, but after *in vitro* growth using the same conditions as for P1 (*Willard-Gallo et al., submitted to Exp Hematol*), an interstitial 6q deletion was detected in one incomplete metaphase cell (Figure 2). No additional metaphase cells carrying a loss of 6q were detectable in the routine annual analysis of this patient's fresh blood; however, the presence of a clonal 6q deletion was confirmed by interphase FISH using a 6q21-located PAC probe (RP3-429G5) on the CD3$^-$CD4$^+$ T cells purified from the patient's frozen blood drawn at diagnosis (Figure 3). Enrichment of the abnormal T-cell population was essential for the success of these experiments due to the low percentage of CD3$^-$CD4$^+$ T cells and/or 6q$^-$ subclones in blood from P2. In contrast to P1, we did not detect a loss of 10p in the CD3$^-$CD4$^+$ T cells from P2 (*data not shown*). These experiments show that at initial diagnosis the CD3$^-$CD4$^+$ T cells from both patients contained a 6q$^-$ subclone and suggest that a 6q abnormality might be a recurrent abnormality in LV-HES.

### *Breakpoints of the 6q and 10p deletions detected in the CD3$^-$CD4$^+$ T cells*

Using a panel of 6q and 10p-specific PAC and BAC probes (Table 1), the chromosomal breakpoints of the previously detected aberrations were mapped by FISH on metaphase cells from P1 and nuclei from P2. Representative metaphase cells from the 6q$^-$, 10p$^-$ and 6q$^-$10p$^-$ subclones in stimulated PBMC from P1

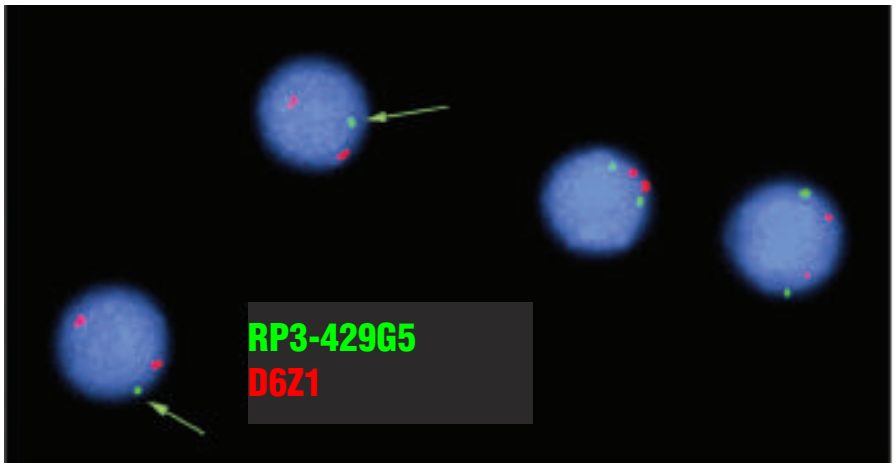


**Figure 3.** Clonality of the 6q deletion in $CD3^{-}CD4^{+}$ T cells from P2. Interphase dual-color FISH on uncultured $CD3^{-}CD4^{+}$ T cells from P2 purified by flow cytometry (98% pure) from blood at initial diagnosis. Co-hybridization of the FITC-labeled RP3-429G5 probe (at 6q21) and the rhodamine-labeled D6Z1 probe (located at the centromere of chromosome 6 and used as internal control), show one green and two red hybridization signals corresponding to 25% of 6q21-deleted nuclei (green arrows).

are shown in Figure 4. In the $6q^{-}$ subclone, the 6q deletion breakpoints were assigned between band 6q13 (RP1-104A17) and band 6q22.1 (RP1-136O14) (Figure 4A and Table 1A). In the $10p^{-}$ subclone, the interstitial deletion was delineated from band 10p11.1 ($D10Z1^{dim}$) to band 10p13 ($RP11\text{-}2K17^{dim}$) (Figure 4B and Table Ib). The location of the 10p13 breakpoint within the RP11-2K17 probe was confirmed using a set of two overlapping BAC probes (Table 1B). In the $6q^{-}10p^{-}$ subclone, the breakpoints of the 10p deletion are identical to the deletion observed in the $10p^{-}$ subclone (Figure 4C and Table 1B). On the other hand, the 6q deletion in the $6q^{-}10p^{-}$ subclone, delineated from band 6q11.1 (D6Z1) to band 6q23.1 (RP3-324N14), is larger than in the $6q^{-}$ subclone (Figure 4C and Table 1A). These results suggest that the $6q^{-}10p^{-}$ subclone was derived from the $10p^{-}$ subclone and not the $6q^{-}$ subclone, and demonstrate that not only was there heterogeneity in the 6q deletion but that these deletions arose independently. In P2, the 6q deletion was defined from band 6q13 (RP3-424L16) to band 6q22.1 (RP3-412I7) by interphase FISH analysis of the enriched $CD3^{-}CD4^{+}$ T cells (Table 1A). Thus, the three distinct 6q deletions (Table 1A) identify a commonly deleted region lying between 6q14.1 (RP1-234P15) and 6q22.1 (RP1-238J17). This shared deleted region contains approximately 164 genes and is 40Mbp long.

### The relationship between cytogenetic changes and the clinical evolution of P1 and P2

The percentage of cells containing the 6q and/or 10p deletion was investigated by interphase FISH on successive blood samples taken at different stages of each patient's disease (Table 2). Blood samples from P1 were tested at diagnosis [P1-yr.0], during the chronic phase controlled by corticotherapy [P1-yr.4] and coincident with the detection of a $CD3^{-}CD4^{+}$ T cell lymphoma [P1-yr.6]. Blood samples from P2 were investigated at diagnosis [P2-yr.0] and after four years of stable clinical remission on corticotherapy (chronic phase) [P2-yr.4]. The $CD3^{-}CD4^{+}$ and

**Table 1A.** Breakpoint delineation of the 6q deletions in P1 and P2 and identification of the shared minimal deletion.

| *6q located PAC probes* | *Chromosome location* | *P1 6q⁻ subclone* | *P1 6q⁻10p⁻ subclone* | *P2 6q⁻ subclone[a]* |
|---|---|---|---|---|
| D6Z1 | Centr 6 | ● | ● | ● |
| RP1-22I17 | 6q12 | ● | ○ | ND |
| RP1-91B17 | 6q12 | ● | ○ | ND |
| RP1-104A17 | 6q13 | ● | ○ | ND |
| RP3-424L16 | 6q13 | ○ | ○ | ● |
| RP1-234P15 | 6q14.1 | ○ | ○ | ○ |
| RP3-429G5 | 6q21 | ○ | ○ | ○ |
| RP1-238J17 | 6q22.1 | ○ | ○ | ○ |
| RP1-136O14 | 6q22.1 | ● | ○ | ○ |
| RP3-412I7 | 6q22.1 | ND | ND | ● |
| RP1-193N13 | 6q22.31 | ● | ○ | ND |
| RP1-293L8 | 6q22.32 | ● | ○ | ND |
| RP3-324N14 | 6q23.1 | ● | ● | ND |
| | | del(6) (q13q22.1) | del(6) (q11.1q23.1) | del(6) (q13q22.1) |

● *no deletion;* ○ *deletion; ND: not done; boxed area: region of minimal deletion.* [a]*The 6q deletion from P2 was delineated by interphase FISH on nuclei from an enriched $CD3^{-}CD4^{+}$ T-cell population.*

**Table 1B.** Breakpoint delineation of the 10p deletion in P1.

| *10p located BAC probes* | *Chromosome location* | *P1 $10p^{-}$ and $6q^{-}10p^{-}$ subclones* |
|---|---|---|
| RP11-398C13[a] | 10p13 | ● |
| RP11-2K17[a] | 10p13 | ● |
| RP11-271M1[a] | 10p13 | ○ |
| RP11-462L8 | 10p11.22 | ○ |
| D10Z1 | Cent 10 | ● |
| RP11-20J15 | 10q11.21 | ● |
| | | del(10)(p11.1p13) |

● *no deletion;* ○ *deletion;* ● *reduced probe signal.* [a]*These BAC clones are contiguous.*

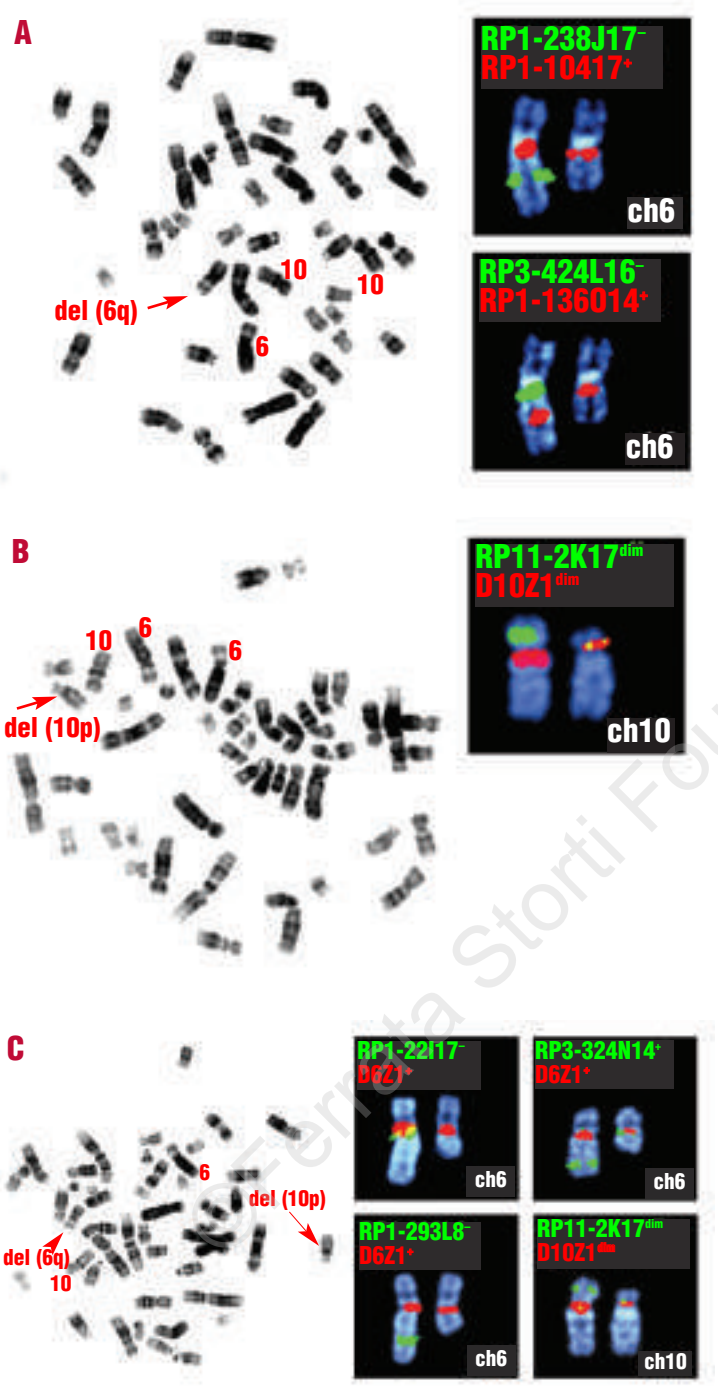


**Figure 4.** Characterization of the P1 subclones using metaphase FISH. The 6q and 10p deletions in the 6q⁻ subclone (A), 10p: subclone (B) and 6q⁻10p⁻ subclone (C) were delineated using metaphase FISH on PMBC stimulated with IL-2, PMA and anti-CD28. A representative pseudo-G-banded metaphase cell and dual-color FISH of DAPI-stained chromosomes 6 and 10 are shown for each subclone. Probes are indicated in each image (text color corresponding to the FISH detection color) along with the signal detected (+ means retained probe signal; – means lost probe signal; dim means diminished probe signal). The 6q13q22.1 deletion (small) is observed in the 6q⁻ subclone (A): the 6q13 breakpoint is detected by the presence of the RP1-104A17 signal and the absence of the RP3-424L16 signal; the 6q22.1 breakpoint is defined by the presence of the RP1-136O14 signal and the absence of the RP1-238J17 signal. The 10p11.1p13 deletion is identically detected in the 10p⁻ subclone (B) and in the 6q⁻10p⁻ subclone (C) by the co-localization of RP11-2K17 (10p13) and D10Z1 (10p11.1) signals. The 6q11.1q23.1 deletion (long) is observed in the 6q⁻10p⁻ subclone (C): the 6q11.1 breakpoint is defined by the presence of the D6Z1 signal (6q11.1) and the absence of the RP1-22I17 signal (6q12); the 6q23.1 breakpoint is defined by the presence of the RP3-424N14 signal (6q23.1) and the absence of the RP1-293L8 signal (6q22.32).



CD3⁺CD4⁺ T cells from each patient were enriched to greater than 96% purity by flow cytometry prior to assessing the frequency of chromosomal abnormalities in the patients' normal and abnormal T-cell populations. This detailed analysis confirmed that the normal CD3⁺CD4⁺ T cells from both patients lacked even a small 6q21 or 10p11.22 deletion. In the CD3⁻CD4⁺ T-cells from P1, the percentage of 6q21-deleted cells, representing both 6q⁻ subsets (the small and large deletions; Table 1A), consistently increased throughout clinical disease progression, peaking at 91% co-incident with the T-cell lymphoma (Table 2). In contrast, the percentage of 6q12-deleted cells, which reflect the 6q⁻10p⁻ subclone only (Table 1A), decreased in parallel with disease progression until these cells were undetectable in the blood sample taken at year 6. Together, these results suggest that the majority of 6q21-deleted cells detected at the time of the lymphoma were in fact from the 6q⁻ subclone (small 6q deletion). In addition, the percentage

**Table 2.** Evolution of the 6q and 10p deleted clones (percent of total $CD3^-CD4^+$ T cells) in successive purified blood samples from P1 and P2.

| *Probe used* | *Chromosome location* | *Subclone(s) represented in the probe-deleted population* | *% of probe-deleted nuclei in the total $CD3^-CD4^+$ T-cell population (a)* | | |
|---|---|---|---|---|---|
| | | | *Chronic phase* | | *T-cell lymphoma* |
| | | | *P1-yr.0 (b)* | *P1-yr.4* | *P1-yr.6* |
| RP3-429G5 | 6q21 | $6q^-$ plus $6q^-10p^-$ | 77% (53%) | 80% (80%) | 91% (91%) |
| RP11-462L8 | 10p11.22 | $6q^-10p^-$ plus $10p^-$ | 54% (37%) | 18% (18%) | < threshold |
| RP1-91B17 | 6q12 | $6q^-10p^-$ | 33% (23%) | 16% (16%) | < threshold |
| | | | *P2-yr.0* | *P2-yr.4* | |
| RP3-429G5 | 6q21 | $6q^-$ | 25% (25%) | 22% (21%) | |

*(a) The percentage of probe-deleted cells was normalized to the percentage of $CD3^-CD4^+$ T cells. In brackets: raw percentage of probe-deleted cells in the sample.*
*(b) This sample was 69% pure $CD3^-CD4^+$ T cells (not purified because of the limited number of available cells).*

of 10p-deleted cells, which include both $10p^-$ and $6q^-10p^-$ subclones, also decreased during disease evolution until they were below the threshold of detection at year 6. In P2, the percentage of 6q21-deleted cells in the $CD3^-CD4^+$ T-cell population remained stable in parallel with this patient's chronic but treatment-responsive disease (25% to 21%; Table 2). These studies underline the apparent importance of the 6q deletion, which was present early and persisted throughout the chronic disease phase in two LV-HES patients, finally emerging in a single subclone in parallel with the $CD3^-CD4^+$ T-cell lymphoma in P1.

### Expression analysis of 6q-located genes

Whole-genome oligonucleotide microarrays were performed on the patients' samples using HG-U133A chips (Affymetrix). Genes located in the commonly deleted 6q14.1-q22.1 region (88 of these genes are present on the U133A chip) were examined in detail by comparing purified $CD3^-CD4^+$ T cells from P1-yr. 6 ($6q^-$ present in 91% of the $CD3^-CD4^+$ T-cells) and P2-yr.0 ($6q^-$ present in 25% of the $CD3^-CD4^+$ T cells) with $CD3^+CD4^+$ T-cells purified from P2-yr.4 as a control. Genes whose expression decreased more than two-fold in the abnormal T cells from P1-yr.6 and P2-yr.0 relative to the control are shown in Table 3. None of the 6q-deleted genes was upregulated in the abnormal T cells.

These changes in gene expression were confirmed and quantified using quantitative real-time PCR (RQ-PCR), employing normal $CD3^+CD4^+$ T cells purified from P2-yr.4 blood as well as from a pool of three healthy donors as controls (Table 3). In general, the loss of expression detected in the arrays was reflected as a loss of expression in RQ-PCR, however there were some discrepancies that are worth mentioning. In the abnormal T-cells from P1, the microarray detected a lower expression of exon 3 than exon 4 of the *FOXO3A* gene (Table 3). An alternatively spliced variant of the *FOXO3A* gene, *FKHRL1P2* lacks exon 4 and is specifically expressed in T-helper cells,[30] suggesting there could be a specific decrease in this alternatively spliced transcript in the cells from P1. Although both techniques did detect a significant decrease in *FOXO3A* gene expression, a specific loss of *FKHRL1P2* expression in the abnormal T cells fom P1 could not be confirmed by RQ-PCR. The array experiments did detect a significant decrease in *BACH2* transcripts in the abnormal T cells from P1 as well as a slight reduction of this transcript in the abnormal T cells from P2. RQ-PCR analysis confirmed that this gene is significantly downmodulated in both patients' abnormal T-cells (Table 3). *BACH2* has been shown to be expressed in B cells,[31] and thus we compared the level of *BACH2* expression in normal $CD4^+$ T cells with $CD20^+$ B cells (>97% pure) isolated from healthy donors. Interestingly, RQ-PCR revealed that while *BACH2* transcripts are expressed in $CD4^+$ T-cells, transcript levels are 3-fold lower than in B cells but 50-fold higher than in P1's and 7-fold higher than in P2's abnormal T-cells (*data not shown*).

The most interesting conclusion drawn from these studies is that the genes whose expression was downregulated in both the microarray and RQ-PCR analysis of abnormal T cells from P2 (*C6ORF37*, *BACH2*, *HMGN3*, *PA26*, *RAGD* and *MARCKS*) also had the greatest changes in the abnormal T cells from P1 (Table 3). Furthermore, the greater frequency of the 6q deletion in $CD3^-CD4^+$ T cells from P1 (91%) compared to those from P2 (25%) was associated with an increase in the number of 6q downmodulated genes as well as frequently lower levels of expression. These data suggest that the changes observed in this subset of 6q-deleted genes can potentially be correlated with the abnormal phenotype and/or malignant progression.

**Table 3.** Decreased expression fold change of 6q14.1-q22.1 located genes.

| GB Acc. No. | Gene description | Locus | Array | RQ-PCR[a] | RQ-PCR[b] |
|---|---|---|---|---|---|
| **P1-yr.6** | | | | | |
| NM_017633 | *C6ORF37* (chromosome 6 open reading frame 37) | 6q14.2 | -15.2 | -37.6±0.3 | -25.4±1.2 |
| NM_021813 | *BACH2* (BTB and CNC homology 1 basic leucine zipper transcription factor 2) | 6q15 | -4.8 | -16.3±2.2 | -17.6±0.5 |
| NM_004242 | *HMGN3* (high mobility group nucleosomal binding domain 3) | 6q14.1 | -2.8 | -5.7±0.4 | -8.8±0.4 |
| NM_014454 | *PA26* (p53 regulated PA26 nuclear protein) | 6q21 | -2.7 | -4.7±0.6 | -12.8±1.4 |
| NM_021244 | *RAGD* (Rag D protein) | 6q15 | -3.9 | -3.8±0.7 | -5.1±0.3 |
| NM_002356 | *MARCKS* (myristoylated alanine-rich protein kinase C substrate) | 6q21 | -3.9 | -2.5±0.5 | -0.5±0.3 |
| NM_006016 | *CD164* (CD164 antigen sialomucin) | 6q21 | -3.0 | -2.5±0.1 | -1.8±0.3 |
| NM_015571 | *SUSP1* (SUMO-1-specific protease) | 6q14.1 | -2.1 | -2.2±0.1 | -3.5±1.6 |
| NM_006813 | *PROL2* (proline rich 2) | 6q15 | -2.2 | -2.1±0.7 | -1.9±0.1 |
| NM_001455 | *FOXO3A* (forkhead box O3A (exon 4))[d] | 6q21 | -2.3 | -2.0±0.1 | -2.0±0.5 |
| NM_020425 | *C6ORF162* (DKFZp586E1923) | 6q15 | -2.6 | -1.9±0.6 | -2.1±0.3 |
| NM_181837 | *ORC3L* (origin recognition complex subunit 3-like (yeast)) | 6q15 | -2.8 | -1.8±0.1 | -1.9±0.1 |
| NM_001455 | *FOXO3A* (forkhead box O3A (exon 3))[c] | 6q21 | -16.0 | -1.7±0.1 | -1.9±0.1 |
| **P2-yr.0** | | | | | |
| NM_004242 | *HMGN3* (high mobility group nucleosomal binding domain 3) | 6q14.1 | -5.0 | -12.9±0.6 | -20.0±1.3 |
| NM_002356 | *MARCKS* (myristoylated alanine-rich protein kinase C substrate)[e] | 6q21 | -9.7 | -11.5±4.4 | -2.5±1.8 |
| NM_017633 | *C6ORF37* (chromosome 6 open reading frame 37) | 6q14.2 | -3.9 | -10.1±0.5 | -6.9±0.1 |
| NM_014454 | *PA26* (p53 regulated PA26 nuclear protein) | 6q21 | -2.3 | -4.6±0.6 | -12.5±1.4 |
| NM_021244 | *RAGD* (Rag D protein) | 6q15 | -2.1 | -4.1±0.2 | -4.1±0.9 |
| NM_021813 | *BACH2* (BTB and CNC homology 1 basic leucine zipper transcription factor 2) | 6q15 | -1.5 | -2.4±0.1 | -5.7±0.9 |

*Array: Mean fold change of all probe sets coding for a specific gene in purified $CD3^-CD4^+$ T cells versus purified $CD3^+CD4^+$ T cells from P2-yr.4. RQ-PCR: Mean fold change from two representative and independent experiments analyzed using RQ-PCR on RNA from purified $CD3^-CD4^+$ T cells versus purified $CD3^+CD4^+$ T-cells ([a]) from P2-yr.4 and ([b]) from a pool of 3 healthy donors. ([c])This probe set hybridizes with both FOXO3A and its alternative spliced variant FKHRL1P2 while ([d]) this probe set hybridizes only FOXO3A. ([e])Variations between replicate samples suggest the instability of this transcript.*

## Discussion

This study has provided evidence that a 6q deletion is recurrent in two LV-HES patients in association with the monoclonal proliferation of their abnormal $CD3^-CD4^+$ T cell clones. Chromosomal abnormalities have been infrequently reported in this discrete pathological entity (summarized in Table 4), because karyotyping was either not performed[20,23] or found to be normal.[15] However, the importance of detecting recurrent chromosomal abnormalities as a diagnostic factor and/or therapeutic target has been illustrated in other types of leukemia emerging from HES.[13] Two major cytogenetic entities have been identified in chronic eosinophilic leukemia: translocations involving the *PDGFRB* gene at 5q33 and a cryptic deletion at 4q12 giving rise to the *FIP1L1-PDGFRA* fusion gene are correlated with a low rate of transformation to acute leukemia and significant clinical responsiveness to tyrosine kinase inhibitors.[32-34] Alternatively, abnormalities involving the 8p11 band (resulting in *FGFR1* gene rearrangements) are frequently detected in pluripotent lymphoid-myeloid stem cells associated with eosinophilia and T-cell lymphoblastic leukemia and correlated with rapid blast transformation and a poor prognosis.[35] Previously published observations indicated that the 6q deletion occurs in only 12-40% of patients with various subtypes of NHL.[5,36] In our study, no unbalanced change on chromosome 6q was detected using interphase FISH to examine the abnormal $CD3^-CD4^+$ T cells from four additional LV-HES patients in our cohort (*data not shown*). The small number of individuals studied is not sufficient to definitively establish the clinical involvement or the prognostic sig-

**Table 4.** Summary of the cytogenetic changes detected in patients with T-cell-mediated HES.

| Study | Sex/ Age | Source of cells | Karyotype |
|---|---|---|---|
| (56) | F/55 | PBL[a] | 47,XX,add(1)(q44),del(6)(q?),add(7)(p15),+8, t(9;14)(p21;q11),del(14)(q?)[25]/46,XX [5] |
| | M/40 | PBL[a] | 47,XY,+5,i(13q),+der(14)t(1.14)(q23;q32), +15,der(17)t(1;17)(q25;q25),-22 [29]/46,XY [19] |
| (15) | M/70 | BM[b] | 46,XY |
| (17) | M/53 | $CD3^+CD4^-$ $CD8^-$ T cells[c] | 46,XY,-16,+der(16)t(16;?)(q22;?) [10] |
| (57) | M/20 | PBMC[d] | 46,XY,+7 [3] |
| Present study | F/20 | PBMC[d] | 46,XX,del(10)(p11p13)/ 46,idem,del(6)(q11q23)/46,XX 46,XX,del(6)(q13q22)([e]) |
| | F/21 | PBMC[d] | del(6)(q13q22),inc/46,XX([e]) |

*[a]Peripheral blood leukocytes; [b]bone marrow; [c]purified by cytometry; [d]peripheral blood mononuclear cells; [e]the refined breakpoints of these deletions and percentage of each subclone are described in the text.*

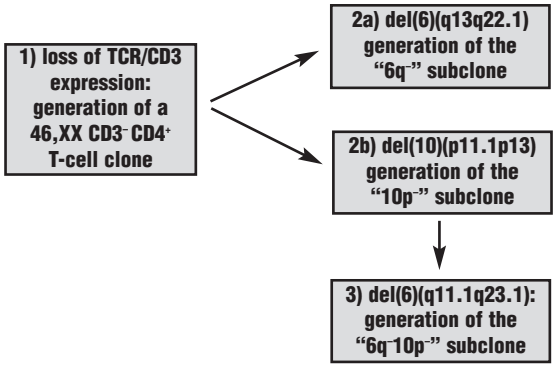


**Figure 5.** The progressive appearance of phenotypic and genetic abnormalities during disease evolution in P1.

nificance of the 6q deletion in LV-HES. However, this aberration has been correlated with distinct biological and hematologic features in specific subsets of lymphoid malignancies, including chronic lymphocytic leukemia[37] and small lymphocytic NHL.[38] In addition, Offit *et al*. associated the deletion of specific 6q regions with different subtypes of NHL, including a 6q21 deletion with high-grade NHL, a 6q23 deletion with low-grade NHL without t(14;18) and a 6q25-27 deletion with intermediate grade NHL.[5] The recurrent 6q deletion reported in various malignancies provided our rationale for investigating its role in the progressive evolution of LV-HES. However, the difficulty of obtaining abnormal metaphase cells for karyotyping in low-grade lymphoproliferative diseases such as LV-HES likely favors an underestimation of the frequency of chromosomal aberrations, including the 6q and 10p deletions. Routine annual karyotyping of our patients did not detect chromosomal aberrations in blood from either patient during the early lymphoproliferative disease phase, making interphase FISH crucial to our study. In addition, increasing the sensitivity by purifying and/or expanding the abnormal cells *in vitro* were effective approaches.

As a model of pre-malignancy, LV-HES provides us with a unique opportunity to investigate chromosomal abnormalities in the early stages of T-cell lymphomagenesis. These patients are frequently diagnosed at a chronic lymphoproliferative phase based on the presence of an aberrant T-cell clone whose lymphokine expression provokes the hypereosinophilia and related cutaneous symptoms.[20] The disease provides a rare opportunity for a genetic follow-up of patients from a pre-cancerous stage through to full-blown malignancy. We propose a timeline for the progressive appearance of biological defects in these patients based on the sequence of clinical events in P1 (Figure 5). Chromosomal abnormalities were detected exclusively in the $CD3^-CD4^+$ T cells, suggesting that loss of TCR/CD3 surface expression preceded the acquisition of an abnormal karyotype in both patients. Subsequent to TCR/CD3 loss, chromosomal abnormalities acquired in P1 followed a pathway of both genetic diversion and progression: the del(6)(q13q22.1) and the del(10)(p11.1p13) occurred independently in individual 46,XX $CD3^-CD4^+$ T cells, giving rise to the $6q^-$ and the $10p^-$ subclones, respectively. Next, the del(6)(q11.1q23.1) occurred in the $10p^-$ subclone, producing a second-generation $6q^-10p^-$ subclone. Our demonstration that the two 6q deletions were acquired independently underscores the importance of this aberration for the survival of the pre-malignant T cells. The coexistence of two 6q deletions of different sizes has been previously reported for an adult ALL patient; however, this study did not establish the sequential evolution of the karyotype.[39] Based on our data, we postulate that the 6q deletion represents an early and critical genetic event in progression of this lymphoproliferative disease to malignancy.

The 6q deletion has occasionally been reported as the sole aberration in lymphoid malignancies,[38,40] however, genetically unbalanced gains and losses including this defect usually develop secondary to disease-specific translocations.[41] Among the secondary events necessary for clonal development, the 6q defect persists throughout tumor development. It has been suggested that in follicular lymphoma associated with a t(14;18) translocation, the 6q deletion initiates one of several cascades of additional genetic changes leading to malignancy.[42] Another study found that the malignant cells from a $CD30^+$ T-cell lymphoma patient, obtained from the primary tumor and after two relapses, may have originated from a common ancestor clone carrying a 6q defect along with trisomy 9.[43] These studies suggest that the inactivation of tumor suppressor genes present in the 6q region are likely important in the early stages of neoplastic progression.

The role of the 6q deletion in LV-HES progression was further investigated by profiling the expression of genes located in the 6q14.1-q22.1 region using microarrays and RQ-PCR. Six of the 88 genes mapped to the 6q region (6.8%) were significantly downregulated in both patients' abnormal T cells. In contrast, no change in the expression of the same genes was observed in $CD3^-CD4^+$ T cells from another LV-HES patient with a normal karyotype (*data not shown*). Furthermore, only 3.4% of the 22,263 genes on the array showed similarly altered and statistically significant expression changes in both patients. These data suggest that the transcriptional alterations

present during both the chronic and malignant phases of LV-HES are more frequent in genes located in the 6q deletion than in the genome as a whole. This observation reinforces our hypothesis that the 6q deletion plays a critical role in the early rather than the later stages of disease progression. Gene expression profiling in association with a 6q defect has not been frequently reported for lymphoid malignancies. Recently, Haslinger *et al*. used microarrays to correlate 17p, 11q and 6q deletions in B-CLL patients with the recurrent downregulation of several genes located in these regions, suggesting a gene dosage effect in disease development.[44] The downregulation of genes located in the deleted 6q13 to 6q21 region corroborates our data since this is the same region that was lost in the abnormal cells from our patients. However, none of the 6q-linked genes downmodulated in Haslinger's study were the same as those with decreased expression in our patients. While we cannot exclude a technical bias, this suggests that similar 6q deletions might induce different abnormalities in B cells and T cells leading to B-CLL or LV-HES.

The identification of 6q-located tumor suppressor gene(s) can be accomplished by analyzing regions of minimal deletion (RMD) using loss of heterozygosity assays or cytogenetic analysis for large groups of patients with lymphoid malignancies. Several studies have identified more than one distinct 6q RMD in an otherwise homogeneous group of patients,[2,3,5,45,46] which suggest tumor-suppressor genes are putatively located at bands 6q15-q16.1,[47] 6q16.3-q21,[2,3,36] 6q23[38,46] and 6q25-q27.[48] Our chromosomal breakpoint analysis of P1 and P2 delineated a large common region of deletion from bands 6q14.1 to 6q22.1, which spans at least two RMD previously found in other lymphoproliferative diseases.

Potentially, the analysis of genes that are downmodulated in conjunction with a 6q loss could also identify candidate tumor suppressor genes. Our microarray experiments detected at least three tumor suppressor candidate genes worthy of further investigation. *C6ORF37* was appreciably downmodulated in the abnormal T cells from P1 and although the function of this gene is unknown it is widely expressed with sequence conservation across species barriers, suggesting an essential cellular role.[49] BACH2 dimerizes with a Maf protein to function as a transcription factor, and mediates the oxidative stress response by inhibiting MARE-dependent gene expression.[50] Furthermore, the loss of BACH2 expression is thought to be a contributing factor in B-cell lymphomagenesis.[31] Studies reported that BACH2 expression occurs only in neurons and B cells;[51] however, *BACH2* mRNA was later detected in the thymus.[31] We have shown that BACH2 is also expressed in mature human $CD4^+$ T cells, and the coupling of its downmodulation with the 6q deletion suggests that genes governed by BACH2 warrant further investigation. PA26 has been shown to be a potent member of the GADD protein family and the main alternative transcript (*PA26-T2*) is known to be upregulated by p53 after genotoxic stress, suggesting its potential role as a tumor suppressor.[52,53] Surprisingly, this gene was downregulated to the same extent in the abnormal T-cells of both patients, despite their different percentages of 6q-deleted cells. We also detected a 2-fold decrease in *p53* expression in both patients' abnormal T-cells, which could in turn decrease *PA26*. p53 haploinsufficiency may contribute to tumorigenesis by a disproportionate alteration (greater than 2-fold) in its transcriptional activity,[54,55] suggesting that *PA26* trancripts could also be reduced via a 6q deletion-independent mechanism resulting from decreased p53 activity.

We took advantage of an exceptional opportunity to follow the progression of an abnormal T-cell clone *in vivo* (*Willard-Gallo et al., submitted to Exp Hematol*) from its pre-malignant state through to the development of full malignancy. These patients afforded us a unique choice to compare an individual's normal T cells ($CD3^+CD4^+$) with the various developmental stages in the life of the abnormal counterparts ($CD3^-CD4^+$). A natural extension of our studies is to use whole genome microarrays as a means of identifying both the significant molecular changes that are consistently correlated with disease progression as well as for the analysis of abnormal T-cells from other LV-HES patients. These data could provide insight into the expression of specific gene sets that are correlated with precise genetic, biological and/or clinical features.

*MR and CS contributed equally to this work. MR, CS and KWG were responsible for designing the study, performing the majority of the experiments, for the analysis and interpretation of the data and for writing the article. FR, LS, and MG were responsible for the clinical analysis and follow-up of the HES patients and for critical revision of the article. HD was responsible for purifying the $CD4^+$ T-cells by flow cytometry. Ch.S contributed his expertise to the microarray experiments and interpretation of these data. PM was involved in successfully treating patient #1's lymphoma by bone marrow transplantation and critical review of the manuscript. All the authors approved the article. The authors declare that they have no potential conflicts of interest.*

*This work was supported by grants from: the Belgian "Fonds National de la Recherche Scientifique" (FNRS-FRSM N° 3.4606.02 and FNRS-Télévie N° 7.4582.03 and 7.4574.03), Fonds Medic and Amis de l'Institut Bordet, Fonds Scientifiques de l'Institut de Pathologie et de Génétique (Loverval, Belgium), Fonds Salus Sanguinis (U.C.L.). KWG is a scientific collaborator of the FNRS-Télévie and MR is a fellow of the FNRS-Télévie.*

*Manuscript received November 19, 2004. Accepted May 15, 2005.*

## References


1. Gerard B, Cave H, Guidal C, Dastugue N, Vilmer E, Grandchamp B. Delineation of a 6 cM commonly deleted region in childhood acute lymphoblastic leukemia on the 6q chromosomal arm. Leukemia 1997;11:228-32.
2. Takeuchi S, Koike M, Seriu T, Bartram CR, Schrappe M, Reiter A, et al. Frequent loss of heterozygosity on the long arm of chromosome 6: identification of two distinct regions of deletion in childhood acute lymphoblastic leukemia. Cancer Res 1998;58:2618-23.
3. Merup M, Moreno TC, Heyman M, Ronnberg K, Grander D, Detlofsson R, et al. 6q deletions in acute lymphoblastic leukemia and non-Hodgkin's lymphomas. Blood 1998; 91:3397-400.
4. Offit K, Jhanwar SC, Ladanyi M, Filippa DA, Chaganti RS. Cytogenetic analysis of 434 consecutively ascertained specimens of non-Hodgkin's lymphoma: correlations between recurrent aberrations, histology, and exposure to cytotoxic treatment. Genes Chromosomes Cancer 1991;3: 189-201.
5. Offit K, Parsa NZ, Gaidano G, Filippa DA, Louie D, Pan D, et al. 6q deletions define distinct clinico-pathologic subsets of non- Hodgkin's lymphoma. Blood 1993; 82:2157-62.
6. Hayashi Y. The molecular genetics of recurring chromosome abnormalities in acute myeloid leukemia. Semin Hematol 2000;37:368-80.
7. Walker GJ, Palmer JM, Walters MK, Hayward NK. A genetic model of melanoma tumorigenesis based on allelic losses. Genes Chromosomes Cancer 1995;12:134-41.
8. Noviello C, Courjal F, Theillet C. Loss of heterozygosity on the long arm of chromosome 6 in breast cancer: possibly four regions of deletion. Clin Cancer Res 1996;2:1601-6.
9. Hyytinen ER, Saadut R, Chen C, Paull L, Koivisto PA, Vessella RL, et al. Defining the region(s) of deletion at 6q16-q22 in human prostate cancer. Genes Chromosomes Cancer 2002; 34:306-12.
10. Sandhu AK, Hubbard K, Kaur GP, Jha KK, Ozer HL, Athwal RS. Senescence of immortal human fibroblasts by the introduction of normal human chromosome 6. Proc Natl Acad Sci USA 1994;91:5498-502.
11. Theile M, Seitz S, Arnold W, Jandrig B, Frege R, Schlag PM, et al. A defined chromosome 6q fragment (at D6S310) harbors a putative tumor suppressor gene for breast cancer. Oncogene 1996;13:677-85.
12. Chusid MJ, Dale DC, West BC, Wolff SM. The hypereosinophilic syndrome: analysis of fourteen cases with review of the literature. Medicine (Baltimore) 1975;54:1-27.
13. Bain BJ. Cytogenetic and molecular genetic aspects of eosinophilic leukaemias. Br J Haematol 2003; 122: 173-9.
14. Cogan E, Schandene L, Crusiaux A, Cochaux P, Velu T, Goldman M. Brief report: clonal proliferation of type 2 helper T cells in a man with the hypereosinophilic syndrome. N Engl J Med 1994;330:535-8.
15. Brugnoni D, Airo P, Rossi G, Bettinardi A, Simon HU, Garza L, et al. A case of hypereosinophilic syndrome is associated with the expansion of a CD3-CD4+ T-cell population able to secrete large amounts of interleukin-5. Blood 1996;87:1416-22.
16. Simon HU, Yousefi S, Dommann-Scherrer CC, Zimmermann DR, Bauer S, Barandun J, et al. Expansion of cytokine-producing CD4-CD8- T cells associated with abnormal Fas expression and hypereosinophilia. J Exp Med 1996;183:1071-82.
17. Kitano K, Ichikawa N, Mahbub B, Ueno M, Ito T, Shimodaira S, et al. Eosinophilia associated with proliferation of CD($3^+$)4-($8^-$) $\alpha\beta^+$ T cells with chromosome 16 anomalies. Br J Haematol 1996;92:315-7.
18. Brugnoni D, Airo P, Tosoni C, Taglietti M, Lodi-Rizzini F, Calzavara-Pinton P et al. $CD3^+CD4^+$ cells with a Th2-like pattern of cytokine production in the peripheral blood of a patient with cutaneous T cell lymphoma. Leukemia 1997;11:1983-5.
19. Bank I, Reshef A, Beniaminov M, Rosenthal E, Rechavi G, Monselise Y. Role of γ/δ T cells in a patient with $CD4^+CD3v$ lymphocytosis, hypereosinophilia, and high levels of IgE. J Allergy Clin Immunol 1998;102:621-30.
20. Simon HU, Plotz SG, Dummer R, Blaser K. Abnormal clones of T cells producing interleukin-5 in idiopathic eosinophilia. N Engl J Med 1999;341: 1112-20.
21. Roufosse F, Schandene L, Sibille C, Kennes B, Efira A, Cogan E, et al. T-cell receptor-independent activation of clonal Th2 cells associated with chronic hypereosinophilia. Blood 1999;94: 994-1002.
22. Roufosse F, Schandene L, Sibille C, Willard-Gallo K, Kennes B, Efira A, et al. Clonal Th2 lymphocytes in patients with the idiopathic hypereosinophilic syndrome. Br J Haematol 2000;109: 540-8.
23. Bank I, Amariglio N, Reshef A, Hardan I, Confino Y, Trau H, et al. The hypereosinophilic syndrome associated with $CD4^+CD3^-$ helper type 2 (Th2) lymphocytes. Leuk Lymphoma 2001; 42:123-33.
24. de Lavareille A, Roufosse F, Schmid-Grendelmeier P, Roumier AS, Schandene L, Cogan E et al. High serum thymus and activation-regulated chemokine levels in the lymphocytic variant of the hypereosinophilic syndrome. J Allergy Clin Immunol 2002;110:476-9.
25. Dutrillaux B, Lejeune J. New techniques in the study of human chromosomes: methods and applications. Adv Hum Genet 1975;5:119-56.
26. Dierlamm J, Wlodarska I, Michaux L, La Starza R, Zeller W, Mecucci C, et al. Successful use of the same slide for consecutive fluorescence in situ hybridization experiments. Genes Chromosomes Cancer 1996;16:261-4.
27. Chomczynski P, Sacchi N. Single-step method of RNA isolation by acid guanidinium thiocyanate-phenol-chloroform extraction. Anal Biochem 1987;162:156-9.
28. Irizarry RA, Hobbs B, Collin F, Beazer-Barclay YD, Antonellis KJ, Scherf U, et al. Exploration, normalization, and summaries of high density oligonucleotide array probe level data. Biostatistics 2003;4:249-64.
29. Beillard E, Pallisgaard N, van dV, V, Bi W, Dee R, van der SE, et al. Evaluation of candidate control genes for diagnosis and residual disease detection in leukemic patients using 'real-time' quantitative reverse-transcriptase polymerase chain reaction (RQ-PCR) - a Europe against cancer program. Leukemia 2003;17:2474-86.
30. DaSilva L, Kirken RA, Taub DD, Evans GA, Duhe RJ, Bailey MA, et al. Molecular cloning of FKHRL1P2, a member of the developmentally regulated fork head domain transcription factor family. Gene 1998;221:135-42.
31. Sasaki S, Ito E, Toki T, Maekawa T, Kanezaki R, Umenai T, et al. Cloning and expression of human B cell-specific transcription factor BACH2 mapped to chromosome 6q15. Oncogene 2000; 19:3739-49.
32. Wilkinson K, Velloso ER, Lopes LF, Lee C, Aster JC, Shipp MA, et al. Cloning of the t(1;5)(q23;q33) in a myeloproliferative disorder associated with eosinophilia: involvement of PDGFRB and response to imatinib. Blood 2003; 102:4187-90.
33. Cools J, DeAngelo DJ, Gotlib J, Stover EH, Legare RD, Cortes J, et al. A tyrosine kinase created by fusion of the PDGFRA and FIP1L1 genes as a therapeutic target of imatinib in idiopathic hypereosinophilic syndrome. N Engl J Med 2003;348:1201-14.
34. Martinelli G, Malagola M, Ottaviani E, Rosti G, Trabacchi E, Baccarani M. Imatinib mesylate can induce complete molecular remission in FIP1L1-PDGFR-a positive idiopathic hypereosinophilic syndrome. Haematologica 2004;89:236-7.
35. Macdonald D, Reiter A, Cross NC. The 8p11 myeloproliferative syndrome: a distinct clinical entity caused by constitutive activation of FGFR1. Acta Haematol 2002;107:101-7.
36. Zhang Y, Matthiesen P, Harder S, Siebert R, Castoldi G, Calasanz MJ, et al. A 3-cM commonly deleted region in 6q21 in leukemias and lymphomas delineated by fluorescence in situ hybridization. Genes Chromosomes Cancer 2000;27:52-8.
37. Cuneo A, Rigolin GM, Bigoni R, De Angeli C, Veronese A, Cavazzini F, et al. Chronic lymphocytic leukemia with 6q- shows distinct hematological features and intermediate prognosis. Leukemia 2004;18:476-83.
38. Offit K, Louie DC, Parsa NZ, Filippa D, Gangi M, Siebert R, et al. Clinical and morphologic features of B-cell small lymphocytic lymphoma with del(6)(q21q23). Blood 1994;83:2611-8.
39. Jackson A, Carrara P, Duke V, Sinclair P, Papaioannou M, Harrison CJ, et al. Deletion of 6q16-q21 in human lymphoid malignancies: a mapping and deletion analysis. Cancer Res 2000; 60:2775-9.
40. Man C, Au WY, Pang A, Kwong YL. Deletion 6q as a recurrent chromosomal aberration in T-cell large granular lymphocyte leukemia. Cancer Genet Cytogenet 2002;139:71-4.
41. Johansson B, Mertens F, Mitelman F. Cytogenetic evolution patterns in non-Hodgkin's lymphoma. Blood 1995; 86: 3905-14.
42. Hoglund M, Sehn L, Connors JM, Gascoyne RD, Siebert R, Sall T, et al. Identification of cytogenetic sub-

groups and karyotypic pathways of clonal evolution in follicular lymphomas. Genes Chromosomes Cancer 2004;39:195-204.
43. Prochazkova M, Chevret E, Beylot-Barry M, Sobotka J, Vergier B, Delaunay M, et al. Chromosomal imbalances: a hallmark of tumour relapse in primary cutaneous CD30+ T-cell lymphoma. J Pathol 2003; 201:421-9.
44. Haslinger C, Schweifer N, Stilgenbauer S, Dohner H, Lichter P, et al. Microarray gene expression profiling of B-cell chronic lymphocytic leukemia subgroups defined by genomic aberrations and VH mutation status. J Clin Oncol 2004; 22:3937-49.
45. Starostik P, Greiner A, Schultz A, Zettl A, Peters K, Rosenwald A, et al. Genetic aberrations common in gastric high-grade large B-cell lymphoma. Blood 2000;95:1180-7.
46. Gaidano G, Hauptschein RS, Parsa NZ, Offit K, Rao PH, Lenoir G, et al. Deletions involving two distinct regions of 6q in B-cell non-Hodgkin lymphoma. Blood 1992;80:1781-7.
47. Hatta Y, Yamada Y, Tomonaga M, Miyoshi I, Said JW, Koeffler HP. Detailed deletion mapping of the long arm of chromosome 6 in adult T- cell leukemia. Blood 1999;93:613-6.
48. Hauptschein RS, Gamberi B, Rao PH, Frigeri F, Scotto L, Venkatraj VS, et al. Cloning and mapping of human chromosome 6q26-q27 deleted in B-cell non- Hodgkin lymphoma and multiple tumor types. Genomics 1998;50:170-86.
49. Lagali PS, Kakuk LE, Griesinger IB, Wong PW, Ayyagari R. Identification and characterization of C6orf37, a novel candidate human retinal disease gene on chromosome 6q14. Biochem Biophys Res Commun 2002;293:356-65.
50. Hoshino H, Kobayashi A, Yoshida M, Kudo N, Oyake T, Motohashi H, et al. Oxidative stress abolishes leptomycin B-sensitive nuclear export of transcription repressor Bach2 that counteracts activation of Maf recognition element. J Biol Chem 2000;275:15370-6.
51. Muto A, Hoshino H, Madisen L, Yanai N, Obinata M, Karasuyama H, et al. Identification of Bach2 as a B-cell-specific partner for small maf proteins that negatively regulate the immunoglobulin heavy chain gene 3' enhancer. EMBO J 1998;17:5734-43.
52. Velasco-Miguel S, Buckbinder L, Jean P, Gelbert L, Talbott R, Laidlaw J, et al. PA26, a novel target of the p53 tumor suppressor and member of the GADD family of DNA damage and growth arrest inducible genes. Oncogene 1999;18:127-37.
53. Kops GJ, Dansen TB, Polderman PE, Saarloos I, Wirtz KW, Coffer PJ, et al. Forkhead transcription factor FOXO3a protects quiescent cells from oxidative stress. Nature 2002;419:316-21.
54. Gottlieb E, Haffner R, King A, Asher G, Gruss P, Lonai P, et al. Transgenic mouse model for studying the transcriptional activity of the p53 protein: age- and tissue-dependent changes in radiation-induced activation during embryogenesis. EMBO J 1997; 16: 1381-90.
55. Santarosa M, Ashworth A. Haploinsufficiency for tumour suppressor genes: when you don't need to go all the way. Biochim Biophys Acta 2004;1654:105-22.
56. Fermand JP, Mitjavila MT, Le Couedic JP, Tsapis A, Berger R, Modigliani R, et al. Role of granulocyte-macrophage colony-stimulating factor, interleukin-3 and interleukin-5 in the eosinophilia associated with T cell lymphoma. Br J Haematol 1993;83:359-64.
57. Roumier AS, Grardel N, Lai JL, Becqueriaux I, Ghomari K, de Lavareille A, et al. Hypereosinophilia with abnormal T cells, trisomy 7 and elevated TARC serum level. Haematologica 2003; 88:ECR24.